



Exploring Chaos and Entanglement in the Hénon–Heiles System Using Squeezed Coherent States

Sijo K. Joseph and Miguel A. F. Sanjuán
*Nonlinear Dynamics, Chaos and Complex Systems Group,
Departamento de Física, Universidad Rey Juan Carlos,
Tulipán s/n, 28933 Móstoles, Madrid, Spain*

Received September 24, 2015

Quantum entanglement in the Hénon–Heiles system is analyzed using the squeezed coherent state. Enhancement of quantum entanglement via squeezing is explored in connection with chaotic and regular dynamics of the system. It is found that the entanglement enhancement via squeezing is implicitly linked to the local structure of the classical phase-space and it shows a clear quantum-classical correspondence. In particular, the entanglement enhancement via squeezing is found to be negligible for a highly chaotic orbit compared to the regular and weakly chaotic orbits, and shows a clear correspondence to the degree of chaos present in the classical initial condition. We believe that these results might be useful to develop efficient strategies to enhance entanglement in quantum systems.

Keywords: Continuous-variable quantum entanglement; quantum chaos; quantum squeezing.

1. Introduction

The Hénon–Heiles system was first studied by the astronomers Michel Hénon and Carl Heiles in 1964, in the context of analyzing the third integral of motion in galactic dynamics [Henon & Heiles, 1964]. This is one of the simplest systems which shows rich dynamical behavior including chaos and escaping dynamics for certain range of energy values. Due to its simplicity and its rich dynamical properties, chaos theorists have extensively explored different classical dynamical aspects of this system [Aguirre *et al.*, 2001; Blesa *et al.*, 2014; Barrio, 2006; Blesa *et al.*, 2012]. In the quantum chemistry community, the Hénon–Heiles system is also widely used to model the polyatomic vibrational spectra and to study the quantum classical correspondence [Pomphrey, 1974]. The initial research work on the quantum Hénon–Heiles system starts from Percival’s postulate on the existence of two kinds of energy levels for a bounded system: one for the regular

orbits and the other one for the chaotic orbits [Percival, 1973]. Further research in this area has clearly established the existence of different types of energy levels termed as “irregular spectrum” and “regular spectrum” which correspond to chaotic and regular orbits respectively [Pomphrey, 1974; Noid *et al.*, 1980]. In the Hénon–Heiles system, Davis, Stechel and Heller [Davis *et al.*, 1980] had analyzed the time evolution of a tensor product coherent state for chaotic and regular initial conditions. They found a clear distinction between the correlation function of the wave function for the chaotic and regular initial conditions. In the celebrated article by Feit, Fleck and Steiger [Feit *et al.*, 1982], they had proposed an extremely efficient computational method to determine the eigenvalues and eigenfunctions of the Schrödinger equation and they have computed the eigenvalues and eigenfunctions of an asymmetric double-well potential and the Hénon–Heiles system with extreme accuracy. In addition to that, Feit and

Fleck [1984] had also analyzed the correspondence between the wavepacket dynamics and chaos in the quantum Hénon–Heiles system. Their split operator algorithm is memory efficient and extremely fast compared with the matrix method. Due to this reason, we use their algorithm to find the time evolution of the initial tensor product squeezed coherent state.

The usual trends in the Quantum Chaos community is to study the energy level statistics and the nodal domain pattern associated with a quantum system as a quantum signature of classical chaos [Berry & Robnik, 1986, 2002]. Periodic orbit theory and the cycle expansion are also considered as one of the major topics [Cvitanović & Eckhardt, 1989]. Improvements in number theory have been made through Quantum Chaos in connection with Berry’s conjecture, which states that the zeros of the Riemann zeta function can be identified as the eigenvalues of a Hermitian operator [Berry & Keating, 1999; Sierra & Rodríguez-Laguna, 2011]. Apart from these lines of research, there is an increased interest in the entanglement dynamics and its quantum-classical correspondence. Theoretically and experimentally it is observed that, there exist a clear relationship between quantum entanglement and classical chaos [Miller & Sarkar, 1999; Ghose & Sanders, 2004; Chaudhury *et al.*, 2009; Lombardi & Matzkin, 2011; Lakshminarayan, 2001].

On the other hand, there is an increased interest in the squeezed quantum states in connection with quantum information processing. In the Jaynes–Cummings model for example, it has been demonstrated that a stronger entanglement between a two-level atom and an electromagnetic field mode can be achieved by using a squeezed state rather than a coherent state as the initial photon state [Furuichi & Mahmoud, 2001]. Interestingly, the entanglement enhancement is observed only when the initial state of the field mode is sufficiently squeezed. In other interesting investigations, the enhancement in entanglement via unequal single-mode squeezing performed separately on the two field modes is studied [Shao *et al.*, 2009; Er *et al.*, 2013]. It is also found that the entanglement persists even in a decohering environment with high temperature when the normal modes are squeezed [Galve *et al.*, 2010]. In addition to that, Wang and Sanders [2003] have analyzed symmetric multiqubit states and they have found a clear relationship between spin squeezing and pairwise entanglement. Most

recently, Beduini and Mitchell [2013] have extended the results of [Wang & Sanders, 2003] to optical fields and they have found a spin-squeezing inequality for photons. Recently, the classically chaotic quantum maps are also explored in connection with quantum computation [Giraud & Georgeot, 2005; Rossini & Benenti, 2008] and it has been found that quantum chaotic maps can efficiently generate pseudorandom states carrying almost maximal multipartite entanglement.

Taking these works into account, it is worthwhile to analyze the effect of squeezing on the entanglement enhancement in the Hénon–Heiles system. Even though the Hénon–Heiles system is widely explored and shows a rich classical dynamical behavior ranging from bounded motion to chaotic and escaping behavior, this system is not explored in connection with the entanglement dynamics. Hence, our goal in this paper is the following. We focus on the entanglement enhancement due to the local squeezing of the wavefunction and its quantum-classical correspondence. It is already known that chaotic orbits can give higher entanglement maxima, while regular orbits give a smaller value [Zhang & Jie, 2008]. Hence the entanglement maxima depends on the nature of the underlying classical dynamics. In this article, we answer the question of entanglement enhancement and its dependency on the underlying regular and chaotic dynamics.

This paper is organized as follows. First, we give a brief theoretical description of the system and a short explanation of all the used numerical tools. Secondly, the classical dynamics of the Hénon–Heiles Hamiltonian is studied in a completely regular phase-space regime and the corresponding quantum entanglement for the squeezed coherent state is analyzed. Finally, the Hénon–Heiles Hamiltonian in the predominantly chaotic phase-space regime is analyzed along with the corresponding quantum entanglement dynamics.

2. Model Description

The classical Hamiltonian of the Hénon–Heiles system can be written as

$$H = \frac{1}{2}(p_x^2 + p_y^2) + V(x, y), \quad (1)$$

where $V(x, y) = \frac{1}{2}(x^2 + y^2) + \lambda(x^2y - \frac{y^3}{3})$ is the two-dimensional Hénon–Heiles potential and λ gives the coupling strength.

In the quantum case, the corresponding Schrödinger equation can be written as:

$$i\hbar \frac{\partial}{\partial t} \psi(x, y, t) = \frac{-\hbar^2}{2m} \nabla^2 \psi(x, y, t) + V(x, y) \psi(x, y, t). \quad (2)$$

The time evolution of the quantum state $\psi(x, y, t)$ is given by

$$\psi(x, y, t) = \hat{U}(t) \psi(x, y, 0). \quad (3)$$

The time evolution of the wave function is performed numerically using the second-order split operator technique. Feit *et al.* [Feit *et al.*, 1982; Feit & Fleck, 1984] have done a detailed analysis of the time evolution of the wavepacket in the Hénon–Heiles potential and we follow their approach.

Since we study the continuous variable entanglement in quantum Hénon–Heiles system, a pure continuous bipartite state can be written as

$$|\psi\rangle_{12} = \int \psi(x, y) |x\rangle |y\rangle dx dy, \quad (4)$$

where $|x\rangle$ and $|y\rangle$ are the continuous basis representation of the position operators of the first and second particles respectively. The reduced density matrix of the first subsystem ρ_1 can be obtained by summing over the second field mode, and it can be represented in terms of the bipartite wave function $\psi(x, y)$, i.e.

$$\rho_1(x, x') = \int \psi(x, y) \psi^*(x', y) dy, \quad (5)$$

where $\rho_1(x, y)$ is the reduced density matrix of the first subsystem in the continuous position basis representation.

To quantify the continuous variable entanglement, we use the von Neumann entropy of the entanglement using the numerical methods proposed by Parker *et al.* [2000] and Bogdanov *et al.* [2006]. The von Neumann entanglement entropy of the reduced density matrix is given by

$$S_{vn}(t) = - \sum \lambda_i \log(\lambda_i), \quad (6)$$

where λ_i are the eigenvalues of the Hermitian kernel $\rho_1(x, x')$. The eigenvalues are computed from the Fredholm type I integral equation of $\rho_1(x, x')$, which is given by

$$\int \rho_1(x, x') \phi_i(x') dx' = \lambda_i \phi_i(x), \quad (7)$$

where λ_i is the eigenvalue of the corresponding Schmidt eigenfunction $\phi_i(x)$.

3. The Squeezed Coherent State

Since the numerical computation is performed using the split operator method, the wavefunction has to be represented in the position basis. Hence, the coordinate representation of the squeezed coherent state is used and different expressions for the coordinate representation of the squeezed coherent state exists [Rai & Mehta, 1988; Fan & VanderLinde, 1989]. Because of the numerical stability for the higher values of the squeezing parameter and due to the relative simplicity of the wavefunction, we prefer the one proposed by Møller, Jørgensen and Dahl [Møller *et al.*, 1996]. Following the definition of Hollenhorst [1979] and Caves [1981] the displacement and squeezing operators can be written as

$$\hat{D}(\alpha_k) = \exp(\alpha_k \hat{a}_k^\dagger - \alpha_k^* \hat{a}_k), \quad (8)$$

$$\hat{S}(\zeta_k) = \exp\left(\frac{1}{2} \zeta_k \hat{a}_k^{\dagger 2} - \frac{1}{2} \zeta_k^* \hat{a}_k^2\right). \quad (9)$$

Then, the squeezed coherent state is defined as

$$|\alpha_k, \zeta_k\rangle = \hat{D}(\alpha_k) \hat{S}(\zeta_k) |0\rangle, \quad (10)$$

where, $\alpha_k = |\alpha_k| e^{i\phi_k}$ and $\zeta_k = |\zeta_k| e^{i\theta_k}$ are complex numbers and α_k are related to the phase-space variables (q_k, p_k) , in the following manner

$$\alpha_k = \frac{1}{\sqrt{2\hbar}} (q_k + ip_k), \quad (11)$$

where $k = 1, 2$, respectively. Following the definition of Møller, Jørgensen and Dahl [Møller *et al.*, 1996], the squeezed coherent state in the position basis can be written as

$$\begin{aligned} \psi(x, \alpha_k, \zeta_k) &= \left(\frac{1}{\pi\hbar}\right)^{1/4} (\cosh r_k + e^{i\theta} \sinh r_k)^{-1/2} \\ &\times \exp\left\{-\frac{1}{2\hbar} \left(\frac{\cosh r_k - e^{i\theta} \sinh r_k}{\cosh r_k + e^{i\theta} \sinh r_k}\right)\right. \\ &\times (x - q_1)^2 + \left.\frac{i}{\hbar} p_1 \left(\frac{x - q_1}{2}\right)\right\}. \end{aligned} \quad (12)$$

The tensor product state $\psi(x, y) = \psi(x, \alpha_1, \zeta_1) \psi(y, \alpha_2, \zeta_2)$ is used to explore the quantum entanglement dynamics for different squeezing parameter values. It is important to mention the quantum-classical correspondence of the classical phase-space variables and the squeezing parameters α_1 and α_2 . Notice that α_k s are the variables associated to a quantum wavefunction and there exist a one-to-one

correspondence between α_k s and the phase-space variables which can be seen in Eq. (11). Thus for every classical initial condition (x, p_x, y, p_y) , a corresponding quantum tensor product wavefunction $\psi(x, y)$ can be found. This correspondence is reflected further in the optical equivalence theorem [Sudarshan, 1963].

4. The Fastest Lyapunov Indicator

In order to measure the degree of chaos associated to a classical initial condition, the Fastest Lyapunov Indicator (FLI) is computed numerically. A dynamical system evolving under the continuous time t obeys the following differential equation

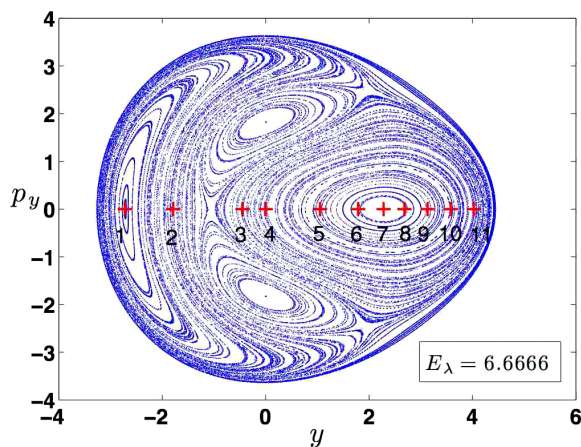
$$\frac{d\mathbf{x}}{dt} = f(\mathbf{x}, t). \quad (13)$$

The variation vector $\boldsymbol{\xi}$ associated with a given trajectory $\mathbf{x}(t)$ obeys the linear differential equation

$$\frac{d\boldsymbol{\xi}}{dt} = Df(\boldsymbol{\xi}, t). \quad (14)$$

The FLI was introduced by Froeschlé and Lega [2000] and it is defined as

$$\text{FLI}(\mathbf{x}(0), \boldsymbol{\xi}(0), t_f) = \sup_{0 < t < t_f} \ln \|\boldsymbol{\xi}(t)\|, \quad (15)$$

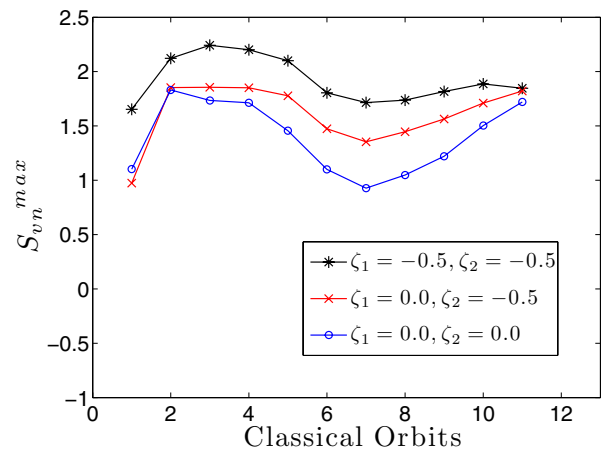


(a)

where t_f is the stopping time. A detailed description on the application of the FLI can be found in [Barrio, 2006] and the references therein.

5. Quantum Entanglement and the Classical Phase-Space Structure

In order to explore the connection between the classical chaos and quantum entanglement in the Hénon-Heiles Hamiltonian, the Poincaré sections of phase-space with energy $E_\lambda = 6.6666$ and $E_\lambda = 13.3333$ are plotted in Figs. 1(a) and 2(a) respectively. Red markers shown inside the Poincaré section indicate the coordinates of the classically centered initial coherent state (CICS). For the notational convenience of the parameters of the CICS, a single parameter ζ is occasionally used to denote the squeezing parameters ($\zeta_1 = \zeta_2$) of the equally squeezed tensor product coherent state. From the previous research works, it can be seen that the classical dynamics of the Hénon-Heiles Hamiltonian is usually studied with the coupling constant $\lambda = 1$, while in the quantum chemistry community the value of the coupling constant $\lambda = 1/\sqrt{80}$ is widely used to study the corresponding quantum system. This is due to the fact that the quantum system is usually analyzed with perturbation theory, so that a small value of the coupling constant λ is preferred



(b)

Fig. 1. The Poincaré section of the Hénon-Heiles system with energy $E = 6.6666$ and $\lambda = 1/\sqrt{80}$ taken at the plane $x = 0$ is shown in (a). The cross symbols inside the Poincaré section denote the initial values of the coherent states which had been chosen to study the entanglement dynamics and the numbers denote the orbit numbers. Hence the entanglement dynamics of a total of 11 orbits are studied. Entanglement dynamics of different classical trajectories are plotted in (b). Blue circles shown in (b) indicate the maximum value of the entanglement for the coherent states and the rest of the different markers show the maximum of the entanglement for the squeezed coherent states. It can be clearly seen that, as the size of the classical tori decreases, the maximum of quantum entanglement entropy decreases and reaches a minimum for the orbit 7. As we move to the right from the orbit 7 to the orbit 8 until the orbit 11, the size of the classical tori increases, so that the maximum of entanglement again starts to increase.

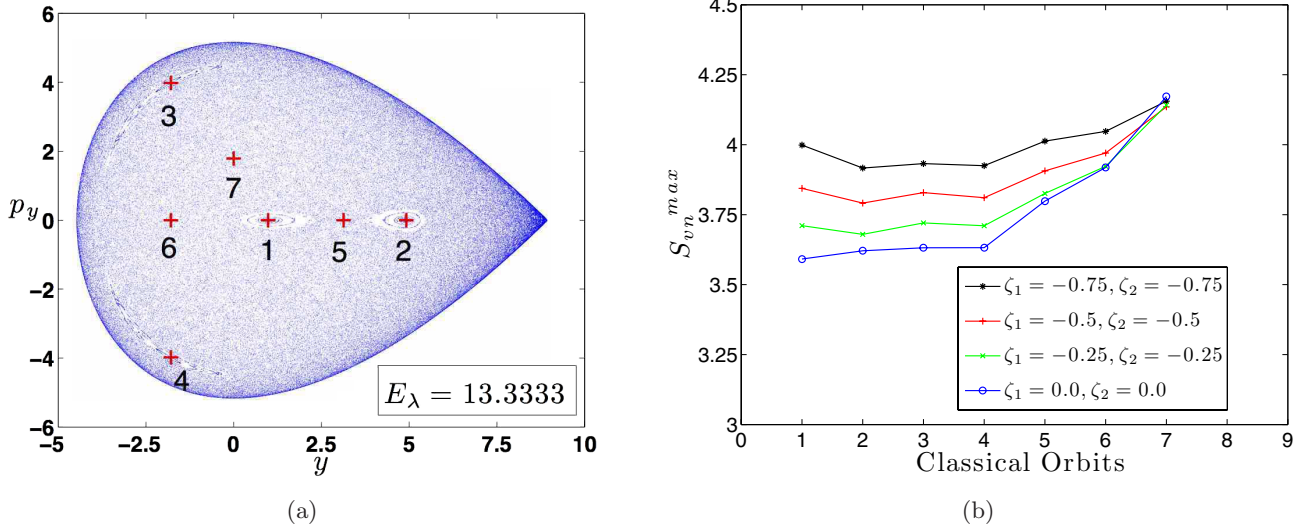


Fig. 2. The Poincaré section of the Hénon–Heiles system with energy $E_\lambda = 13.3333$ and coupling constant $\lambda = 1/\sqrt{80}$ taken at the plane $x = 0$ is shown in (a). The cross markers inside the Poincaré section denote the initial values of the coherent state which had been chosen to study the entanglement dynamics and the numbers denote the corresponding orbit numbers. Here the orbits from 1 to 4 are regular and the rest of the orbits (from 5 to 7) are chaotic. Blue circles shown in (b) indicate the maximum value of the entanglement for the coherent state and the rest of the different markers show the entanglement maxima for the squeezed coherent states. We can clearly see that for the squeezed coherent state, the chaotic orbit has the higher entanglement maximum compared to the regular ones. Notice that, the highly chaotic orbit 7 has a negligible entanglement enhancement compared to the weakly chaotic orbits and the regular orbits.

to obtain a better numerical accuracy. In our case, we do not use the perturbation theory to study the quantum system, so that the small value of λ is not a numerical constraint here. It is known that the Hénon–Heiles Hamiltonian obeys a scaling invariance under the phase-space variable transformation $Q_1 = \lambda x$ and $P_1 = \lambda p_x$, $Q_2 = \lambda y$ and $P_2 = \lambda p_y$, and the energy will be scaled like $E_\lambda = E/\lambda^2$. Here E_λ corresponds to the energy associated with the Hamiltonian $H(p_x, q_x, p_y, q_y, \lambda)$ [see Eq. (1)] while E corresponds to the energy associated with the Hamiltonian $H(P_1, Q_1, P_2, Q_2, \lambda = 1)$ which is extensively explored by the classical chaos community. Hence $E_\lambda = 6.6666$ corresponds to $E = 1/12$ and $E_\lambda = 13.3333$ corresponds to $E = 1/6$, which are the numerical values widely used by the classical chaos community.

5.1. Regular phase-space and quantum entanglement

We first look into the entanglement dynamics in the regular phase-space case. For the classical energy $E_\lambda = 6.6666$ and coupling constant $\lambda = 1/\sqrt{80}$, the classical phase-space of the Hénon–Heiles system is regular, and the Poincaré section consists of tori of different sizes [see Fig. 1(a)]. This has

already been pointed out by Hénon and Heiles [1964]. In the quantum regime we choose a tensor product squeezed coherent state centered around the markers given inside the Poincaré section which is shown in Fig. 1(a). Then, the entanglement dynamics is analyzed during the time evolution of these wavepackets and the entanglement maxima are plotted in Fig. 1(b). It is observed that the entanglement maxima increases as we go from the smaller inner classical tori to the bigger outer tori. In other words, the entanglement production depends on the nature of the underlying classical trajectory. This can be easily seen from Fig. 1(b), and it is clear that the entanglement production is larger for the larger tori and smaller for smaller tori. These results are in accordance with the result of the Pullen–Edmonds Hamiltonian as pointed out by Zhang and Jie [2008]. In their analysis, they already had shown that for the coherent states the entanglement maximum is directly associated with the size of the classical tori on the Poincaré section. Here, we can clearly see that those results are not only true for the coherent states but also true for the squeezed coherent state in the Hénon–Heiles system. Notice that, as the tori size increases, the entanglement enhancement via squeezing gets smaller.

5.2. Chaotic phase-space and quantum entanglement

Here, a detailed analysis on the entanglement dynamics and its quantum classical correspondence is performed on the chaotic phase-space. It is widely known that, for energy $E_\lambda = 13.3333$ and coupling constant $\lambda = 1/\sqrt{80}$, the classical phase-space of the Hénon–Heiles system is predominantly chaotic. In the Poincaré section shown in Fig. 2(a), the classical tori fill only a small region of the phase-space. This has already been pointed out by Hénon and Heiles [1964]. It can be seen that in the quantum regime, an initial tensor product coherent state becomes entangled during its time evolution, consequently the value of the von Neumann entropy saturates after a specific interval of time. In Fig. 2(b) the entanglement maxima are plotted for the squeezed coherent states corresponding to different classical orbits. From Fig. 2(b) it can be seen that, the entanglement maxima are higher for the chaotic orbit and smaller for the regular orbit. In other words, the entanglement production depends on the dynamical nature of the underlying classical trajectory. These results are again in accordance with the result pointed out by Zhang and Jie [2008] on the Pullen–Edmonds Hamiltonian. Notice that, it can be seen from Figs. 2(a) and 2(b) that the orbits 5–7 are in the middle of the chaotic sea, thus the enhancement of entanglement due to squeezing is smaller in these cases, compared with the rest of the regular orbits.

We can also see that the enhancement of entanglement via squeezing is higher in regular orbits (orbits 1 to 4) compared to the rest of the chaotic orbits. For the highly chaotic orbit 7, the enhancement of entanglement is extremely small compared with all other orbits. Even chaotic orbits 5 and 6 have larger entanglement enhancement due to squeezing, compared to the highly chaotic orbit 7.

To have a clear picture of the difference in entanglement enhancement, orbits 1 and 7 from the mixed phase-space are plotted in Fig. 3. It can be seen from Fig. 3(a) that the entanglement enhancement via squeezing is higher for the regular orbit 1 of the mixed phase-space as compared to the highly chaotic orbit 7 shown in Fig. 3(b). This crucial difference in the entanglement enhancement in the chaotic orbits can be understood in terms of the degree of chaos present in these individual orbits.

Since FLI is a good tool to measure the degree of chaos, in Fig. 4 the FLI is plotted for all the seven orbits of the chaotic phase-space [see the corresponding orbits Fig. 2(a)]. It is important to mention that, FLI simply measures the maximum of the divergence of the nearby trajectories in the phase-space for a given time interval t_f , hence it is always a positive definite quantity. It is already known that FLI increases linearly with respect to time for a regular orbit while there exist an exponential growth for a chaotic orbit. From Fig. 4, it can be seen that orbit 7 has a higher degree of chaos,

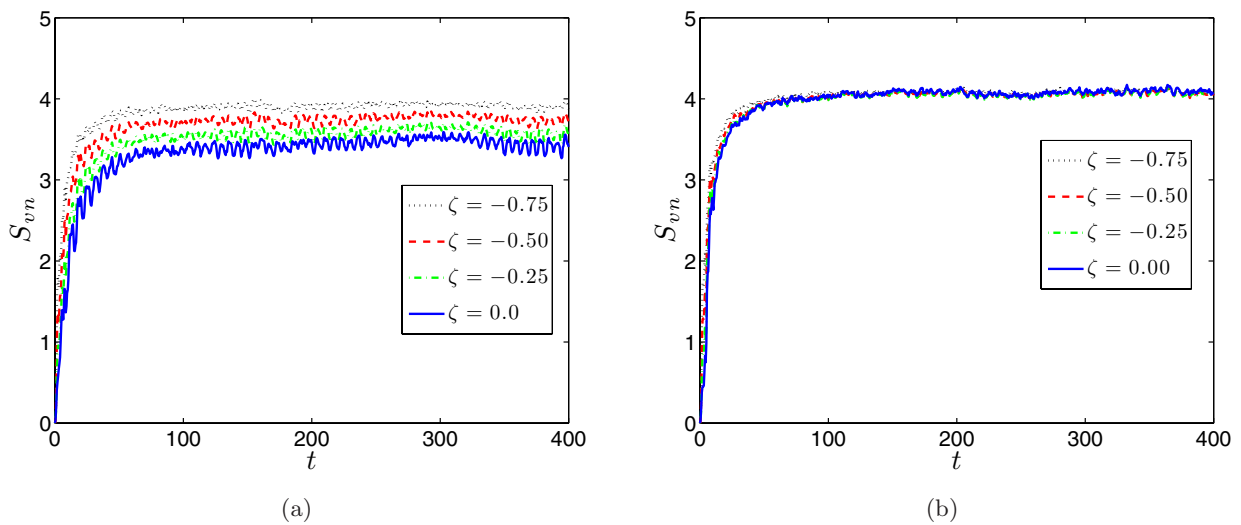


Fig. 3. The entanglement dynamics of the squeezed coherent state of the regular orbit [orbit 1 which is shown in Fig. 2(a)] and the chaotic orbit [orbit 7 which is shown in Fig. 2(a)] are shown in (a) and (b) respectively. Note that both orbits have the classical energy $E_\lambda = 13.3333$. From these figures, it can be seen that the entanglement enhancement via squeezing is negligible for the chaotic orbit as compared to the regular orbit.

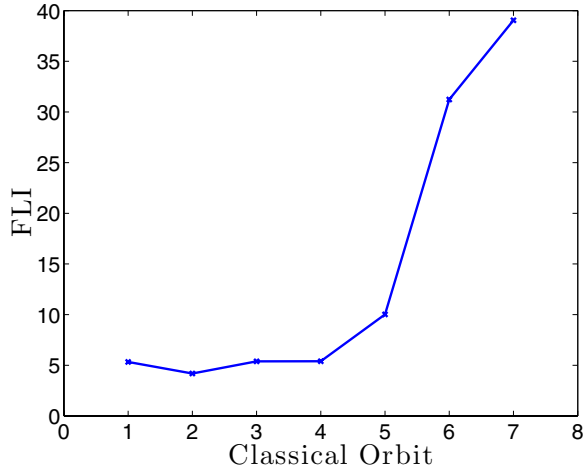


Fig. 4. This figure shows the Fastest Lyapunov Indicator with the stopping time $t_f = 400$ for all the initial conditions shown in Fig. 2(a). It can be clearly seen that FLI is higher for the chaotic orbit and smaller for the regular orbit. Notice that, orbit 7 has the higher valued FLI compared to the other chaotic orbits 5 and 6. This clearly explains the observed quantum entanglement maxima of the chaotic orbits.

since FLI is higher in this case. Hence, it can be argued that the entanglement maximum is directly related to the degree of chaos present in the classical trajectory. Note that we can have a one-to-one correspondence between the FLI in Fig. 4 and the entanglement maximum shown in Fig. 2(b). In each orbit the FLI and the entanglement are increasing gradually. From this observation, we can easily explain the observed difference in the entanglement enhancement of the chaotic orbits. It is observed that the Møller's wavefunction given in Eq. (12) can give a position squeezed coherent state for the negative values of the squeezing parameter. Since the position squeezed wavefunction is more localized in the configuration space and there is a good one-to-one correspondence between FLI and the entanglement maxima of the squeezed coherent states as compared to the coherent state, it is important to note that the highly chaotic orbit 7 can give a higher value of entanglement maximum even without squeezing. It is already known that quantum chaos can define an upper bound in the entanglement dynamics. Thus, the obtained dynamical entanglement of the highly chaotic orbit 7 is closer to the upper bound. Further action of the squeezing operation does not enhance the entanglement beyond this value. This will explain the negligible entanglement enhancement of the chaotic orbit 7, while in the case of chaotic orbits 5 and 6,

the degree of chaos is smaller and the entanglement maximum is not closer to the upper bound. Thus, applying the squeezing can enhance the entanglement in these orbits up to the allowed upper bound. It is to be noted that the chaotic orbits always have a higher entanglement maximum compared to the regular orbit and the quantum classical correspondence is always maintained. The quantum density spectrum of the squeezed coherent state can shed light on these results. Quantum density spectrum ρ_{nn} is computed from the Fourier transform of the autocorrelation function of the time evolved wavefunction. In Fig. 5, the quantum density spectrum of the squeezed coherent state is plotted with classical energy $E = 13.3333$ and coupling constant $\lambda = 1/\sqrt{80}$. Figures 5(a) and 5(b) show the density spectrum for the regular orbit 1 of the mixed phase-space with the squeezing parameters $\zeta = 0.0$ and $\zeta = -0.75$ respectively. At the same time Figs. 5(c) and 5(d) show the density spectrum for the chaotic orbit 7 with the squeezing parameters $\zeta = 0.0$ and $\zeta = -0.75$ respectively. It can be seen that, in Fig. 5(a) the quantum density contains less number of frequency components, when the squeezing is applied the density spectrum contains more additional frequencies with a smaller amplitude. The same is true for the classically chaotic orbit 7 shown in Figs. 5(c) and 5(d). Hence it is clear that the squeezing operation can increase the number of frequency components in the quantum density spectrum. From the semi-classical analysis, it is already known that the quantum frequency spectrum is intriguingly linked to the EBK tori in the phase-space [Martens & Ezra, 1985]. It has been seen that the increased number of frequency components due to squeezing operation in the chaotic case is minimal compared to the regular ones. These frequency components can be easily related to the classical tori in the phase-space. In the classical sense, the squeezed coherent state can be considered as a squeezed Gaussian ensemble of classical initial conditions around a mean phase-space point. Thus it can be said that the squeezing operation samples more regions in the phase-space and there exist a saturation value of the available phase-space region. Once the orbit is highly chaotic, the accessible phase-space region is already higher and squeezing operation cannot enhance this accessible region considerably, while the weakly chaotic orbit can access little more available phase-space region. In the case of regular orbit a smaller squeezing

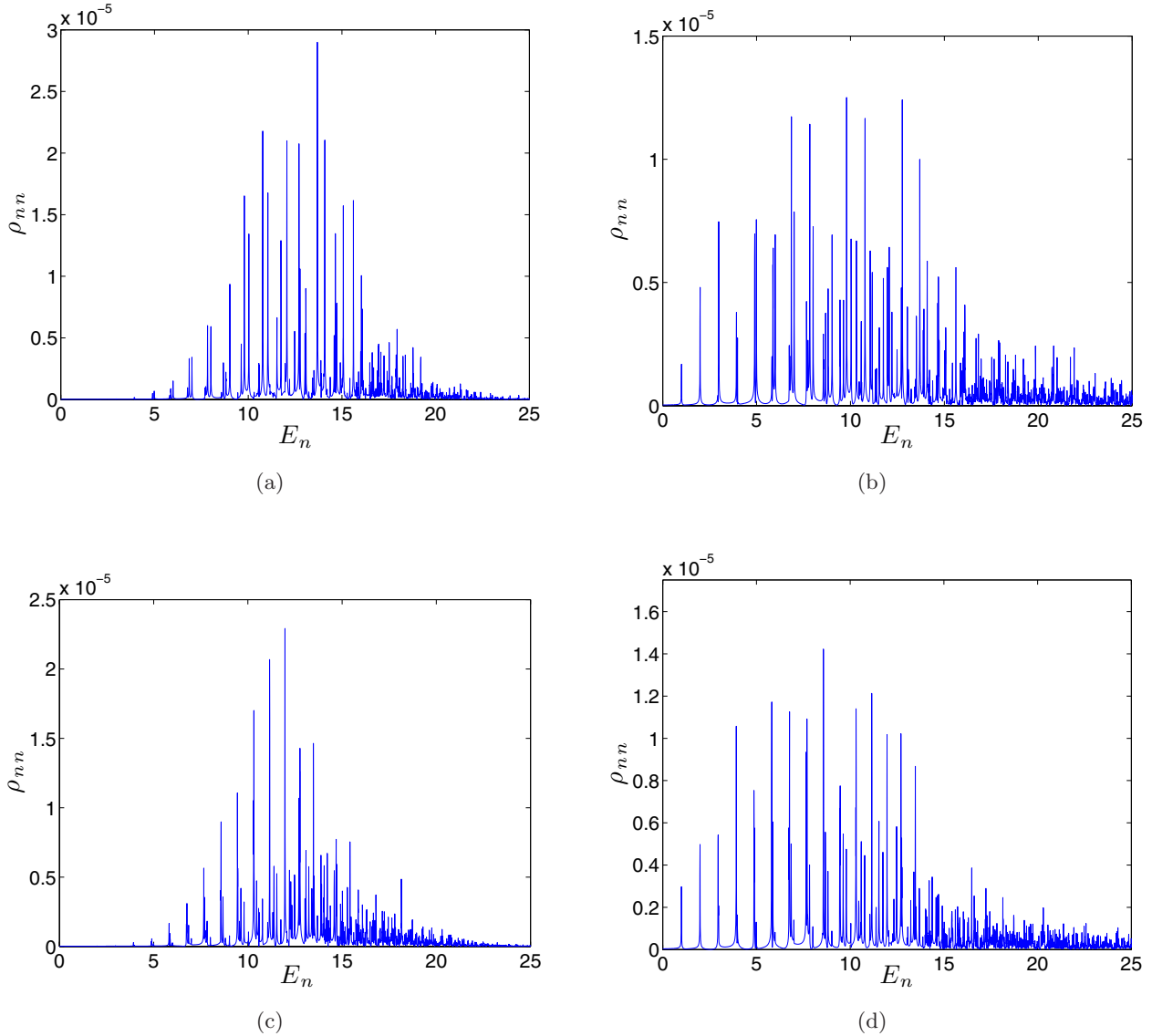


Fig. 5. The quantum density spectrum for the squeezed coherent state with classical energy $E = 13.3333$ and coupling constant $\lambda = 1/\sqrt{80}$. (a) and (b) The density spectrum for the regular orbit 1 with the squeezing parameters $\zeta = 0.0$ and $\zeta = -0.75$ respectively. At the same time, (c) and (d) show the density spectrum for the chaotic orbit 7 with the squeezing parameters $\zeta = 0.0$ and $\zeta = -0.75$ respectively. The quantum density of the entangled coherent state contains lesser frequency components, as shown in (a). When the squeezing is applied, more additional frequencies appear in the quantum density spectrum, as seen in (b). The same is true for the classically chaotic orbit 7 shown in (c) and (d).

can lead the classical trajectories into more accessible regions of the phase-space since the trajectory occupies a smaller region of the available phase-space. This again explains the observed difference in the entanglement enhancement dependence on the degree of chaos present in the orbits. In short, our observation is that for the regular orbit the entanglement enhancement via squeezing is higher compared to the chaotic orbit. If the orbit is highly chaotic, then the entanglement enhancement is negligible. Feingold and Peres [1985] had

explored the propagators associated to the chaotic and regular orbits. They had found that the rms time average of a chaotic propagator is nearly uniformly spread in the Hilbert space. On the other hand the propagator from a regular state is localized in a subset of states and it almost does not reach other parts of the Hilbert space. In the context of the wavepacket dynamics a chaotic initial condition can visit more regions in the Hilbert space compared to a regular initial condition. In the pure classical regime, it is already known that the chaotic

initial conditions contain more spectral components in the Fourier transform of the classical trajectory than the regular ones [Zhang & Jie, 2008]. Martens and Ezra [1985] had computed the semiclassical energy levels and the action variables using EBK quantization based upon the Fourier representation of the invariant tori in the quasiperiodic regime. Hence, in the classical regime, the classical frequency components are intriguingly related to the underlying classical tori [Zhang & Jie, 2008]. As the number of frequency components increase, the accessible phase-space region increases for the corresponding classical initial condition. This is evident due to the fact that the chaotic orbit has the more accessible phase-space region. Bipartite entanglement enhancement and its connection to the accessible phase-space region had already been explored by the authors in the recent article [Joseph *et al.*, 2014b]. Authors had also found an analytical method to find the effect of squeezing on short time entanglement entropy [Joseph *et al.*, 2014a] in the chaotic Hamiltonian including the Hénon–Heiles Hamiltonian. In this study, we further explore the degree of chaos in each orbit and we have analyzed the corresponding difference in entanglement enhancement. We see that as the degree of chaos increases, the enhancement in the entanglement maxima is small. This is a more general result compared to our previous analysis [Joseph *et al.*, 2014b], more specifically, in this manuscript the degree of chaos present in the individual orbit has been taken into account.

6. Conclusions

Quantum entanglement of the squeezed coherent state in the Hénon–Heiles Hamiltonian is explored. It is found that in a completely regular phase-space, the entanglement maximum depends on the size of the underlying classical tori. In other words, entanglement maximum depends on the distance of the given torus from the Poincaré–Birkhoff hyperbolic fixed point. In the case of a chaotic phase-space, it is found that the squeezing can considerably enhance the entanglement of the regular initial conditions compared to the chaotic initial conditions. At the same time, for the highly chaotic initial conditions the enhancement of entanglement is negligible compared to the regular and less chaotic orbits. A clear correspondence between the von Neumann entropy of entanglement and the Fastest Lyapunov Indicator is found, and the connection between the degree

of chaos and the entanglement enhancement via squeezing is explored.

Acknowledgment

This work was supported by the Spanish Ministry of Science and Innovation under project number FIS2013-40653-P.

References

- Aguirre, J., Vallejo, J. C. & Sanjuán, M. A. F. [2001] “Wada basins and chaotic invariant sets in the Hénon–Heiles system,” *Phys. Rev. E* **64**, 066208.
- Barrio, R. [2006] “Painting chaos: A gallery of sensitivity plots of classical problems,” *Int. J. Bifurcation and Chaos* **16**, 2777–2798.
- Beduini, F. A. & Mitchell, M. W. [2013] “Optical spin squeezing: Bright beams as high-flux entangled photon sources,” *Phys. Rev. Lett.* **111**, 143601.
- Berry, M. V. & Robnik, M. [1986] “Statistics of energy levels without time-reversal symmetry: Aharonov–Bohm chaotic billiards,” *J. Phys. A: Math. Gen.* **19**, 649–668.
- Berry, M. V. & Keating, J. P. [1999] “The Riemann zeros and eigenvalue asymptotics,” *SIAM Rev.* **41**, 236–266.
- Berry, M. V. & Robnik, M. [2002] “Statistics of nodal lines and points in chaotic quantum billiards: Perimeter corrections, fluctuations, curvature,” *J. Phys. A: Math. Gen.* **35**, 3025–3038.
- Blesa, F., Seoane, J. M., Barrio, R. & Sanjuán, M. A. F. [2012] “To escape or not to escape, that is the question — Perturbing the Hénon–Heiles Hamiltonian,” *Int. J. Bifurcation and Chaos* **22**, 1230010-1–9.
- Blesa, F., Seoane, J. M., Barrio, R. & Sanjuán, M. A. F. [2014] “Effects of periodic forcing in chaotic scattering,” *Phys. Rev. E* **89**, 042909.
- Bogdanov, A., Bogdanov, Y. & Valiev, K. [2006] “Schmidt modes and entanglement in continuous-variable quantum systems,” *Russ. Microelectron.* **35**, 7–20.
- Caves, C. M. [1981] “Quantum-mechanical noise in an interferometer,” *Phys. Rev. D* **23**, 1693–1708.
- Chaudhury, S., Smith, A., Anderson, B. E., Ghose, S. & Jessen, P. S. [2009] “Quantum signs of chaos in a kicked top,” *Nature* **461**, 768–771.
- Cvitanović, P. & Eckhardt, B. [1989] “Periodic orbit quantization of chaotic systems,” *Phys. Rev. Lett.* **63**, 823–826.
- Davis, M. J., Stechel, E. B. & Heller, E. J. [1980] “Quantum dynamics in classically integrable and non-integrable regions,” *Chem. Phys. Lett.* **76**, 21–26.
- Er, C. H., Chung, N. N. & Chew, L. Y. [2013] “Threshold effect and entanglement enhancement through local squeezing of initial separable states in continuous-variable systems,” *Phys. Scripta* **87**, 025001.

- Fan, H.-Y. & VanderLinde, J. [1989] “Simple approach to the wave functions of one- and two-mode squeezed states,” *Phys. Rev. A* **39**, 1552–1555.
- Feingold, M. & Peres, A. [1985] “Regular and chaotic propagators in quantum theory,” *Phys. Rev. A* **31**, 2472–2476.
- Feit, M., Fleck, J. A. & Steiger, A. [1982] “Solution of the Schrödinger equation by a spectral method,” *J. Comput. Phys.* **47**, 412–433.
- Feit, M. D. & Fleck, J. A. [1984] “Wave packet dynamics and chaos in the Hénon–Heiles system,” *J. Chem. Phys.* **80**, 2578–2584.
- Froeschlé, C. & Lega, E. [2000] “On the structure of symplectic mappings. The fast Lyapunov indicator: A very sensitive tool,” *Celest. Mech. Dyn. Astron.* **78**, 167–195.
- Furuichi, S. & Mahmoud, A. A. [2001] “Entanglement in a squeezed two-level atom,” *J. Phys. A: Math. Gen.* **34**, 6851.
- Galve, F., Pachón, L. A. & Zueco, D. [2010] “Bringing entanglement to the high temperature limit,” *Phys. Rev. Lett.* **105**, 180501.
- Ghose, S. & Sanders, B. C. [2004] “Entanglement dynamics in chaotic systems,” *Phys. Rev. A* **70**, 062315–062319.
- Giraud, O. & Georgeot, B. [2005] “Intermediate quantum maps for quantum computation,” *Phys. Rev. A* **72**, 042312–042315.
- Henon, M. & Heiles, C. [1964] “The applicability of the third integral of motion: Some numerical experiments,” *Astron. J.* **69**, 73.
- Hollenhorst, J. N. [1979] “Quantum limits on resonant-mass gravitational-radiation detectors,” *Phys. Rev. D* **19**, 1669–1679.
- Joseph, S. K., Chew, L. Y. & Sanjuán, M. A. F. [2014a] “Effect of squeezing and Planck constant dependence in short time semiclassical entanglement,” *Eur. Phys. J. D* **68**, 238.
- Joseph, S. K., Chew, L. Y. & Sanjuán, M. A. F. [2014b] “Impact of quantum-classical correspondence on entanglement enhancement by single-mode squeezing,” *Phys. Lett. A* **378**, 2603–2610.
- Lakshminarayanan, A. [2001] “Entangling power of quantized chaotic systems,” *Phys. Rev. E* **64**, 036207.
- Lombardi, M. & Matzkin, A. [2011] “Entanglement and chaos in the kicked top,” *Phys. Rev. E* **83**, 016207.
- Martens, C. C. & Ezra, G. S. [1985] “Ebk quantization of nonseparable systems: A Fourier transform method,” *J. Chem. Phys.* **83**, 2990–3001.
- Miller, P. A. & Sarkar, S. [1999] “Signatures of chaos in the entanglement of two coupled quantum kicked tops,” *Phys. Rev. E* **60**, 1542–1550.
- Møller, K. B., Jørgensen, T. G. & Dahl, J. P. [1996] “Displaced squeezed number states: Position space representation, inner product, and some applications,” *Phys. Rev. A* **54**, 5378–5385.
- Noid, D. W., Koszykowski, M. L., Tabor, M. & Marcus, R. A. [1980] “Properties of vibrational energy levels in the quasi periodic and stochastic regimes,” *J. Chem. Phys.* **72**, 6169–6175.
- Parker, S., Bose, S. & Plenio, M. B. [2000] “Entanglement quantification and purification in continuous-variable systems,” *Phys. Rev. A* **61**, 032305.
- Percival, I. C. [1973] “Regular and irregular spectra,” *J. Phys. B: At. Mol. Opt. Phys.* **6**, L229.
- Pomphrey, N. [1974] “Numerical identification of regular and irregular spectra,” *J. Phys. B: At. Mol. Opt. Phys.* **7**, 1909.
- Rai, J. & Mehta, C. L. [1988] “Coordinate representation of squeezed states,” *Phys. Rev. A* **37**, 4497–4499.
- Rossini, D. & Benenti, G. [2008] “Robust and efficient generator of almost maximal multipartite entanglement,” *Phys. Rev. Lett.* **100**, 060501-1–4.
- Shao, B., Xiang, S. & Song, K. [2009] “Quantum entanglement and nonlocality properties of two-mode Gaussian squeezed states,” *Chin. Phys. B* **18**, 418.
- Sierra, G. & Rodríguez-Laguna, J. [2011] “ $H = xp$ model revisited and the Riemann zeros,” *Phys. Rev. Lett.* **106**, 200201–200203.
- Sudarshan, E. C. G. [1963] “Equivalence of semiclassical and quantum mechanical descriptions of statistical light beams,” *Phys. Rev. Lett.* **10**, 277–279.
- Wang, X. & Sanders, B. C. [2003] “Spin squeezing and pairwise entanglement for symmetric multiqubit states,” *Phys. Rev. A* **68**, 012101.
- Zhang, S.-H. & Jie, Q.-L. [2008] “Quantum-classical correspondence in entanglement production: Entropy and classical tori,” *Phys. Rev. A* **77**, 012312.